Melting of aluminum with ideal or defect lattice: Molecular dynamics simulations with accounting of electronic heat conductivity

V S Krasnikov and A E Mayer

Chelyabinsk State University, Bratiev Kashirinykh Street 129, Chelyabinsk 454001, Russia

E-mail: vas.krasnikov@gmail.com

Abstract. In this work, the atomistic simulations of rapid melting of aluminum are performed. We use the two-temperature approach separately describing the ionic and electronic subsystems of crystal. Both ideal and defect states of initial lattice are considered. The dependence of melting temperature on pressure is investigated in the simulations of thermal equilibrium establishment in the systems with plate interphase boundaries. Non-equilibrium melting of aluminum is studied in simulations with the constant rate of heat energy supply. The maximal temperatures of overheated material before complete melting are obtained in dependence of energy supply rate. Presence of initial defects of lattice substantially decreases the overheating of material. Electronic heat conductivity significantly accelerates the thermal equilibrium establishment in systems with interphase boundaries and decreases the drop of temperature after beginning of melting in the systems with constant rate of heating.

1. Introduction

The generation of shock waves with extremely high deformation rates on its front is realized today by short laser irradiation [1–4], the prospective method for generation of such waves is high-current electron beam [5, 6]. During the fast release of irradiation energy in thin layer of target the overheated state of substance can be realized due to high rate of heating. Also, thermal expansion of substance leads to the onset of high mechanical stresses, so subsequent melting occurs in conditions of compressed substance. These two factors require an accurate description in order to predict the initial shock front shape or to interpret the results of back surface movement registering after shock reflecting from it. The propagation of shock wave can be directly modeled by molecular dynamics (MD) simulations including the situation of stress pulse excitation by an irradiation [7–10]. Another way for description of this situation is a usage of well calibrated continuum models that allow simulating more realistic space and time scales; the parameters of the continuum model can be obtained in MD simulations. This method combining two-scale simulations is actively developed through last decades. The problem of fast melting of substance is widely studied in atomistic simulations starting from pioneering works [11, 12]; in first off which, the finite overheating temperature and influence of lattice defects on it was studied; the second paper was devoted to investigation of dependence of melting temperature on pressure. Nowadays, two tendency in MD simulations are formed: part of works uses the atomistic simulations for determination of the kinetics coefficient [13–18], which

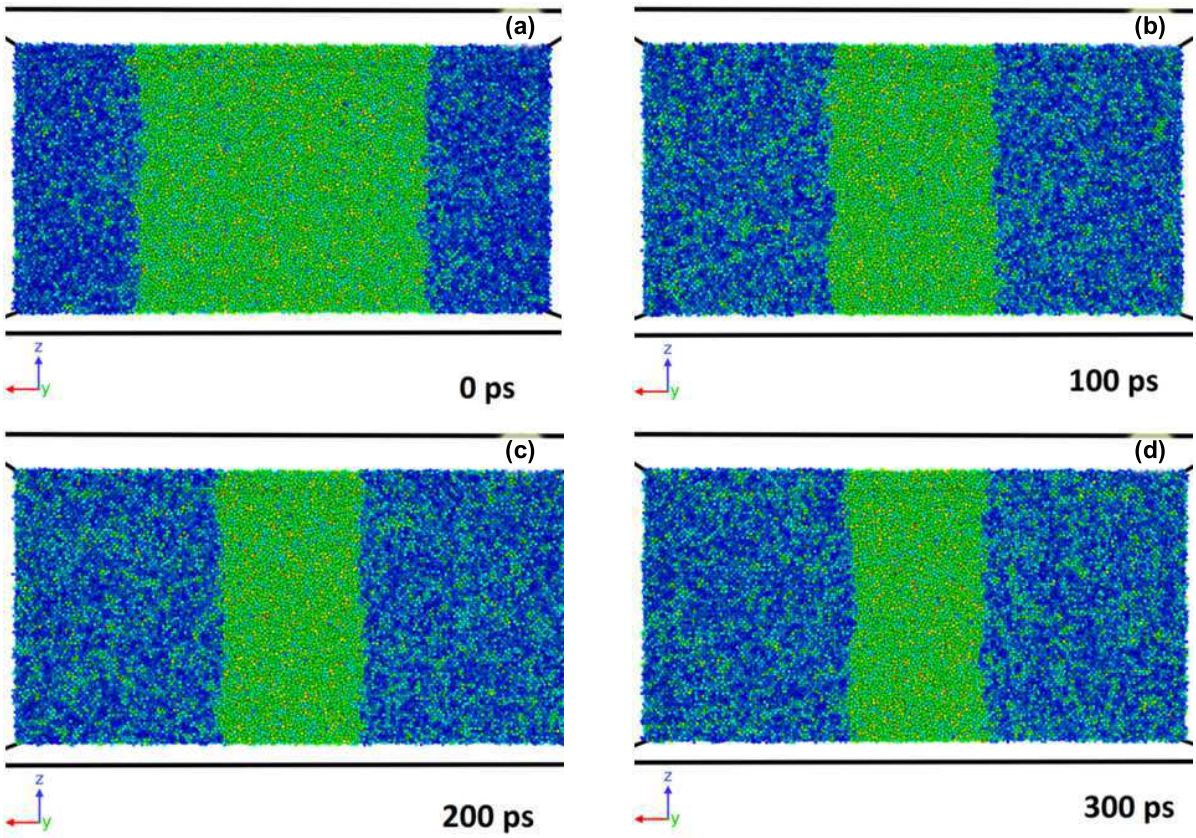

Figure 1. Location of plane boundaries of melt and solid aluminum in dependence on time. Atoms of solid are primarily colored by blue, liquid—by green.

controls the propagation velocity of the interface between phases, part—for the nucleation rate of melting or crystallization sites [18–20].

Heat transfer in metals occurs mainly through the electronic subsystem of crystal. We account the electronic heat conductivity in metals in our calculations in order to account realistic rates of heat supply or removal in aluminum. Presence of the lattice defects can provoke the substantial difference in behavior of systems during melting due to the increased energy of atoms in defect regions. We, also, account three types of possible lattice defects, which in our calculations are pre-existing before melting void, dislocation network and grain boundaries.

2. Melting of aluminum with ideal lattice

Molecular dynamics simulations of melting kinetics is performed with the LAMMPS package [21], which is built with the GPU [22] and TTM [23–26] libraries. The TTM libraries extend the LAMMPS for accounting of the electronic heat conductivity through solution of heat conductivity equation for the electronic subsystem of metal. The parameters of the electronic heat conductivity model are taken from [26, 27] for temperature of 1000 K: heat capacity of electronic gas $C_e = 1.3 \times 10^5$ J m^{-3}K^{-1}, heat conductivity coefficient $\kappa_e = 110$ W m^{-1}K^{-1}, intensity of heat exchange between ions and electrons $g_p = 3 \times 10^{17}$ W m^{-3}K^{-1}. The interaction of atoms is reproduced by EAM potential, which was especially developed to accurately describe melting of aluminum [28]. We use the OVITO [29] tool for visualization of the obtained atom distributions and the centrosymmetrical parameter [30] to distinguish the solid and melt parts in these distributions.

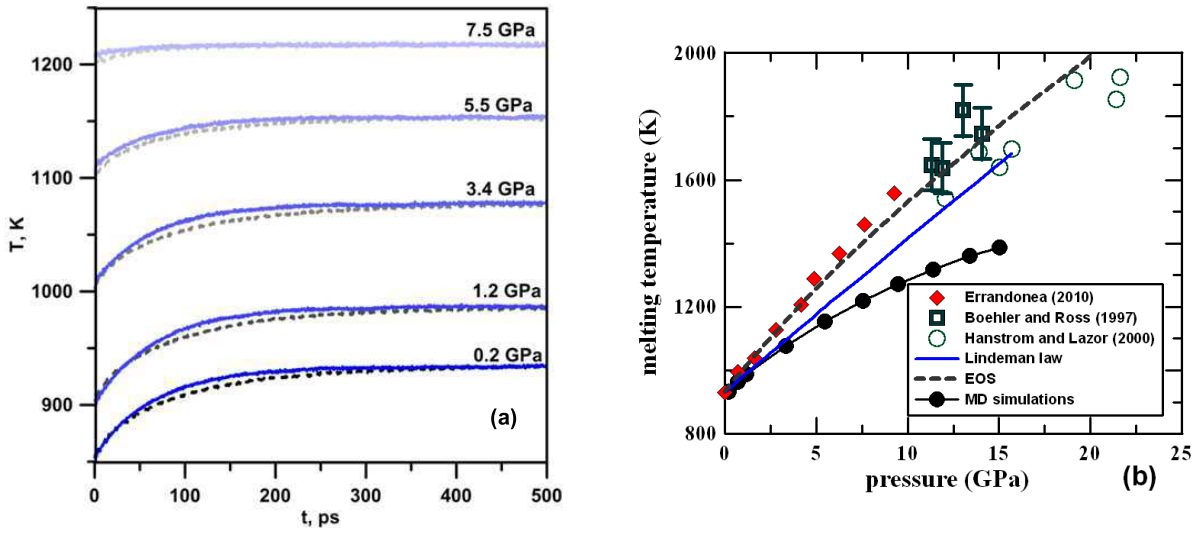

Figure 2. (a) Establishment of temperature in area with phase boundaries: solid and dashed lines correspond to calculations with and without electronic heat conductivity respectively. (b) Dependence of melting temperature on pressure in system in comparison with experimental data: Errandonea—[31], Boehler and Ross—[32], Hanstrom and Lazor—[33], Lindeman law—[34], and EOS—melting curve calculated on equation-of-sate model [35,36] applied to aluminum.

The melting curve of aluminum in dependence on the pressure is studied in the statement with partially melted area with two plane phase boundaries [14, 15, 18]. In this series of calculations we use a rectangular area with the size $40 \times 20 \times 20$ nm^3 that corresponds to one million of atoms. The melt, which is occupied a central part of the area, and the surrounding solid are at the same temperature in the initial state of system. After that, the system is maintained in the adiabatic state with constant volume. The steady temperature and pressure, which are achieved in the system during a thermal establishment, are further used as one point on the melting curve of aluminum

During a movement of flat front between the liquid and solid phases the volume of melt can increase or decrease depending on initial temperature and pressure in the system. If the initial temperature in the calculation area is lower the melting temperature of substance at given pressure, than the crystallization of central melted zone occurs and its volume decreases (figure 1). During the process of crystallization phase front retains the flat shape, but asperities and cavities with amplitude of 3–4 interatomic distances can form randomly along the Oyz cross section on it. The average over the system temperature rises due to the release of latent heat of melting in the crystallizing layer near the phase front (figure 2). With the course of time the average temperature in system achieves the steady-state value after that the translatory movement of phase boundaries ceases, but the asperities and cavities continue to forms at it (figure 1). When the initial temperature in the area exceeds the melting temperature, the average temperature of system decreases and the volume of melt increases; stored heat energy is spent for latent heat of melting. The steady-state temperatures are the same for systems both with initial temperature lower and higher than melting temperature at fixed final pressure in area. Movement of crystallization front occurs with release of latent heat of melting in thin layer of atoms near phase boundary, thus part of these atoms belonging to solid phase possess the higher kinetic energy in comparison with other atoms of solid distant from the phase boundary. The distribution of averaged along Oyz plane temperature of ions demonstrates local maxima near the phase boundary with an amount of 50–70 K for any time moment; the thickness of this layers is of

about 2–4 nm. Temperature of electrons is more homogeneous and changes in the system no more than 10 K near the peaks of ions temperature. The difference between temperatures of atoms and electrons in these peaks typically is lower than 50 K. It is interesting, how the rate of heat removal from this thin atom layer is to affect the velocity of crystallization front motion. In order to investigate the impact of heat conductivity onto establishment of steady-state temperature we perform additional calculations without electronic heat conductivity. When the heat transfer is realized only through ionic subsystem of crystal the rate of heat conductivity substantially decreases that provokes more prolonged establishment of heat balance in system (figure 2). For calculations with very different initial and final temperatures the times obtained in the simulation with the electronic thermal conductivity and without it can differ by 50–60%.

The obtained value of the melting temperature at the pressure of 0.2 GPa is equal to 933 K, which corresponds to the melting point of aluminum at zero pressure. Results obtained in this work with used potential for aluminum do not well correspond with both experimental data and Lindeman law; the MD curve of melting point vs. temperature has the bend, which differs from other data in the figure 2b. The melting curve obtained from MD calculations demonstrates the increase in the melting temperature T_{m} (K) with the increase in pressure P (GPa) in accordance with the following approximation

$$T_{\mathrm{m}} = 933 + 46.9P - 1.3P^2 + 0.012P^3.$$

The second series of calculations is aimed to the study of the kinetics of melting at different rates of energy supply. In this case, the computational area is a cube with sides of 24.5 nm, and there are 846 000 atoms in the area. The system is heated at a constant zero pressure with a constant rate of energy supply starting from 900 K through the increase of kinetic energy of ions.

The supply of heat with constant rate leads initially to the practically linear increase in temperature; here the curve slope is defined by heat capacity of systems (figure 4). A slight deviation from the linearity appears to be associated with the formation of the liquid phase nuclei, but the formation of critical nuclei does not occur at the initial stage of process (figure 4). The size of forming areas of liquid phase increases together with growth of temperature; and at some moment the critical nucleus is formed, which does not later disappear and serves as the fixed center of substance melting. The formation of critical nuclei and the onset of substance melting lead to a sharp drop in the temperature of the area due to conversion of thermal energy of the atoms in the latent heat of melting (figure 4). Rise of the temperature is resumed after the complete melting of substance in area. Increase of the energy supply rate leads to increase of maximum temperature reaching before the start of melting and to deepening of minimum in the temperature dependencies, because the heat supply partially covers the energy required for melting.

Initial curve slope is somewhat smaller in the case of calculations with the electronic heat conductivity, which is connected with the contribution of the heat capacity of electrons. The maximal overheating is approximately the same for both types of calculations. A considerable difference takes place near the bottom of the energy drop, where the MD system without electronic subsystem demonstrates lower temperature. Analysis of the mean density evolution reveals that the complete melting occurs earlier in this case (without accounting of electrons), which is reflected on the temperature behavior. The later completion of melting for system with electrons can be caused by the fact that the electronic thermal conductivity distributes the excess thermal energy over the all volume of the system. In the case of absence of the electronic thermal conductivity, this thermal energy is concentrated inside the solid phase between the melting sites that accelerates the melting.

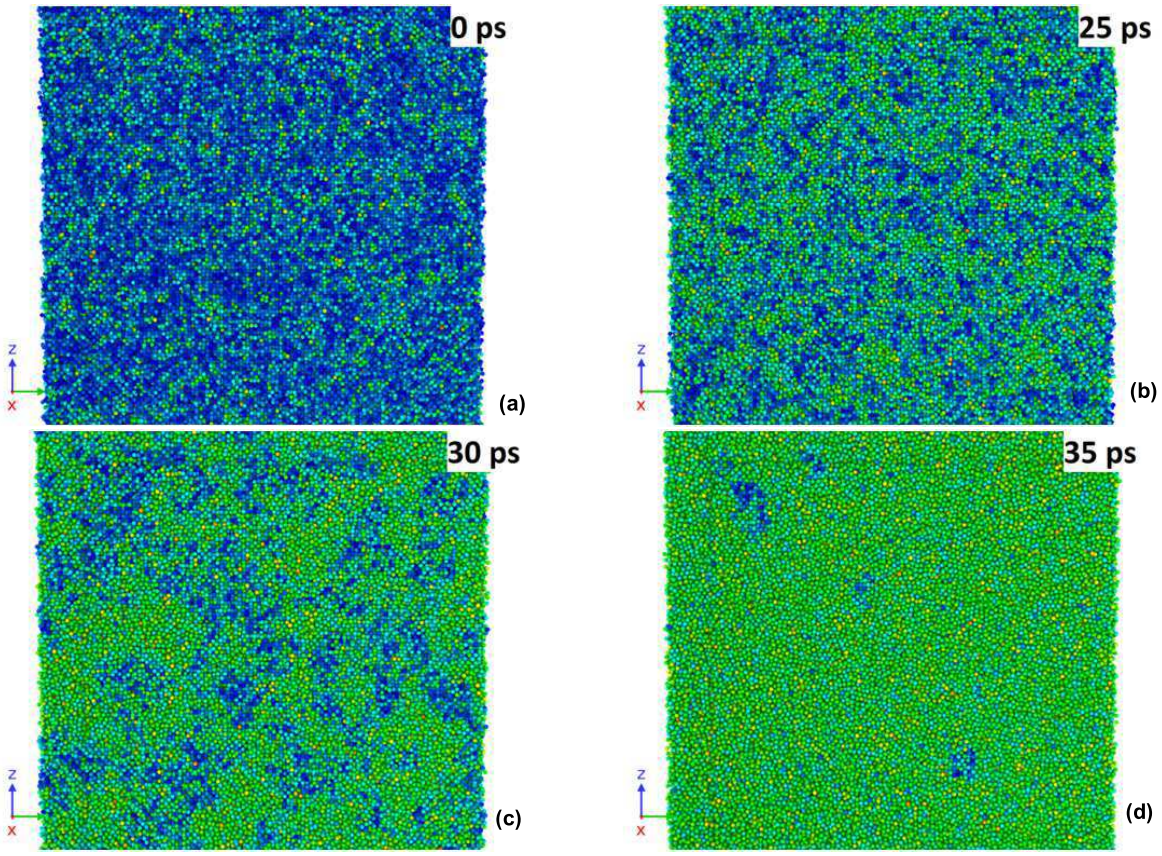

Figure 3. Melting of aluminum with ideal lattice. Various moments of time are presented under heating with constant rate of 15 PW/kg. Atoms of solid are primarily colored by blue, liquid—by green.

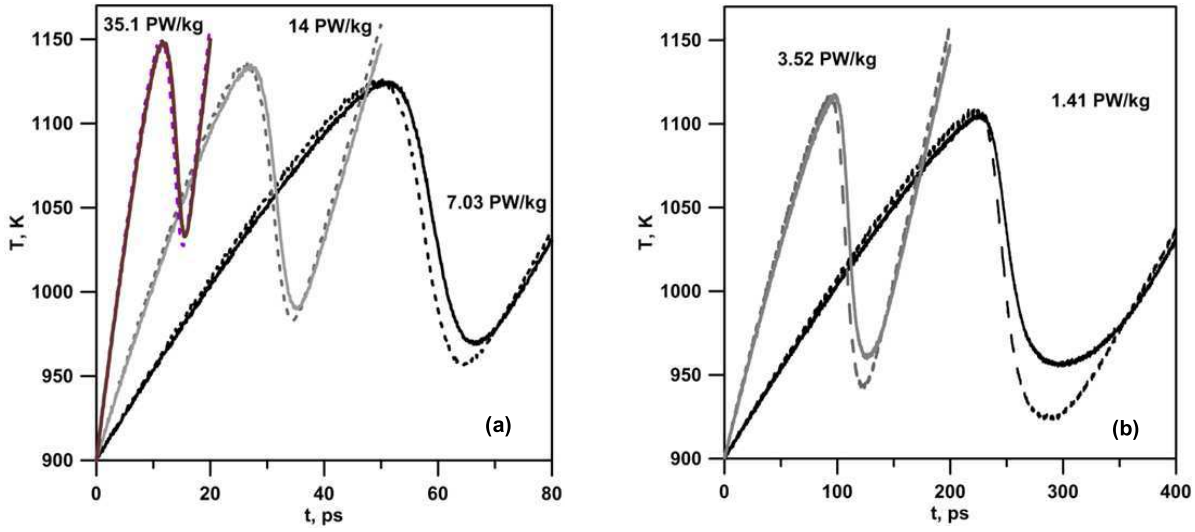

Figure 4. Time dependencies of temperature under heating with constant rate. Solid lines correspond to calculations with electronic heat conductivity, dashed—without it.

3. Melting of aluminum containing initial defect structure

The atomistic modeling of heating of systems containing the initial defect structure is performed to study the role of various lattice defects on melting and overheating of substance. Three types

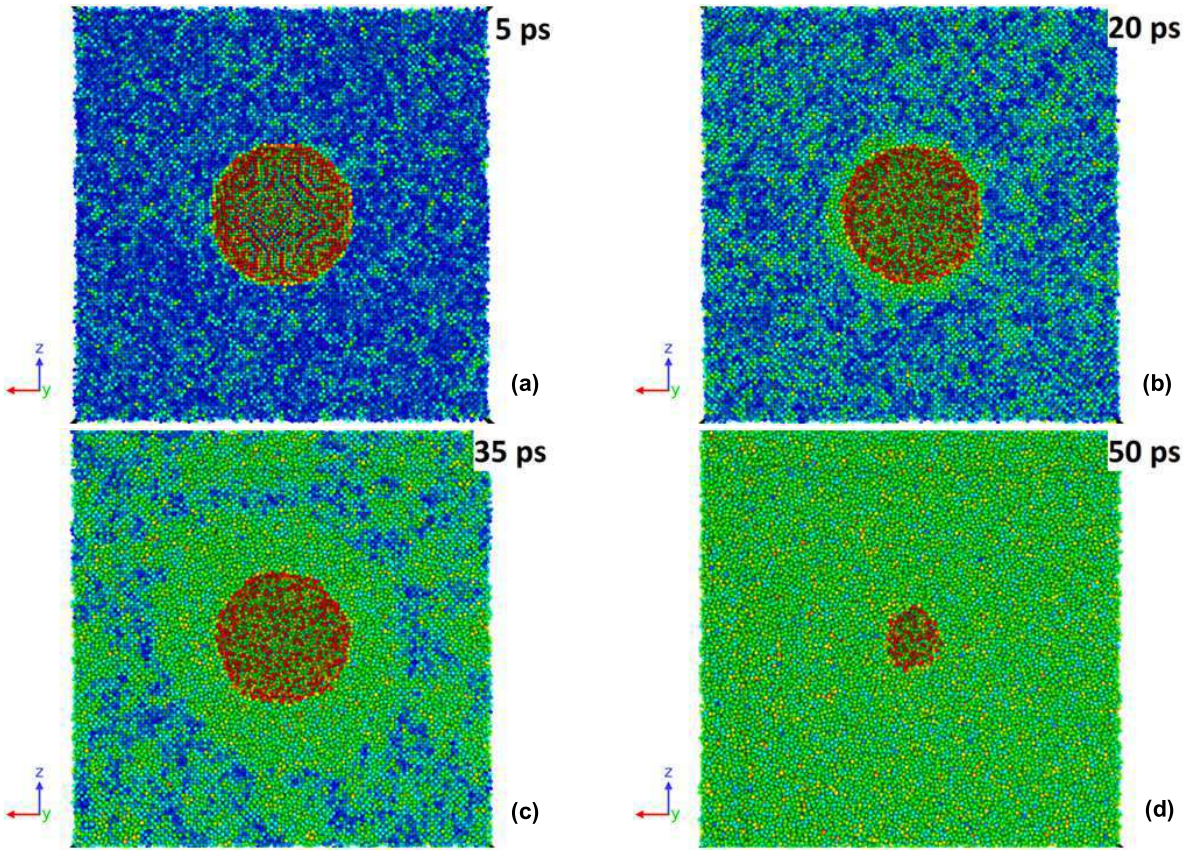

Figure 5. Melting of aluminum containing initial void. Various moments of time are presented under heating with constant rate of 15 PW/kg. Atoms of solid are primarily colored by blue, liquid—by green.

of defect structure of crystal are chosen as the objects of investigation: dislocation network, grain boundaries and void. Void in the material is created by removal of atoms in the spherical area located in the center of the system (figure 5). The initial dislocation structure is formed during the compression of system with preliminarily created void. The defect structure consisting mainly of stacking faults bounded by partial dislocations and of small portion of vacancies is formed as a result of compression (figure 6). Samples with the grain boundaries are created through simulation of the metal melt crystallization onto several misoriented nucleation centers placed randomly into the melt. As a result, the nanosized grains are formed with a typical size of tens of nanometers and a thickness of the grain boundary of 3–5 interatomic distances (figure 7). The systems created with help of these three methods are characterized by varying amounts of defect atoms relative to the total number of atoms in the system; for spherical void this number is minimal and equal to about 0.4%, for the system with dislocation network it is 4.9%, for the sample with grain boundaries it reaches 6.8%.

When the heating of the area with the initial void is modeled, the formation of liquid phase nuclei occurs quite homogeneously throughout the area, however, the maximum concentration of nuclei is observed at the surface of the void (figure 5). These nuclei coalescing during further heating form a spherical region around the void of substance experienced transition to the liquid state; at the same time melting courses in other points of substance. After the full transition of substance in area to liquid state the void starts collapsing under the action of surface tension forces. Time dependencies of temperature for this series of calculations slightly

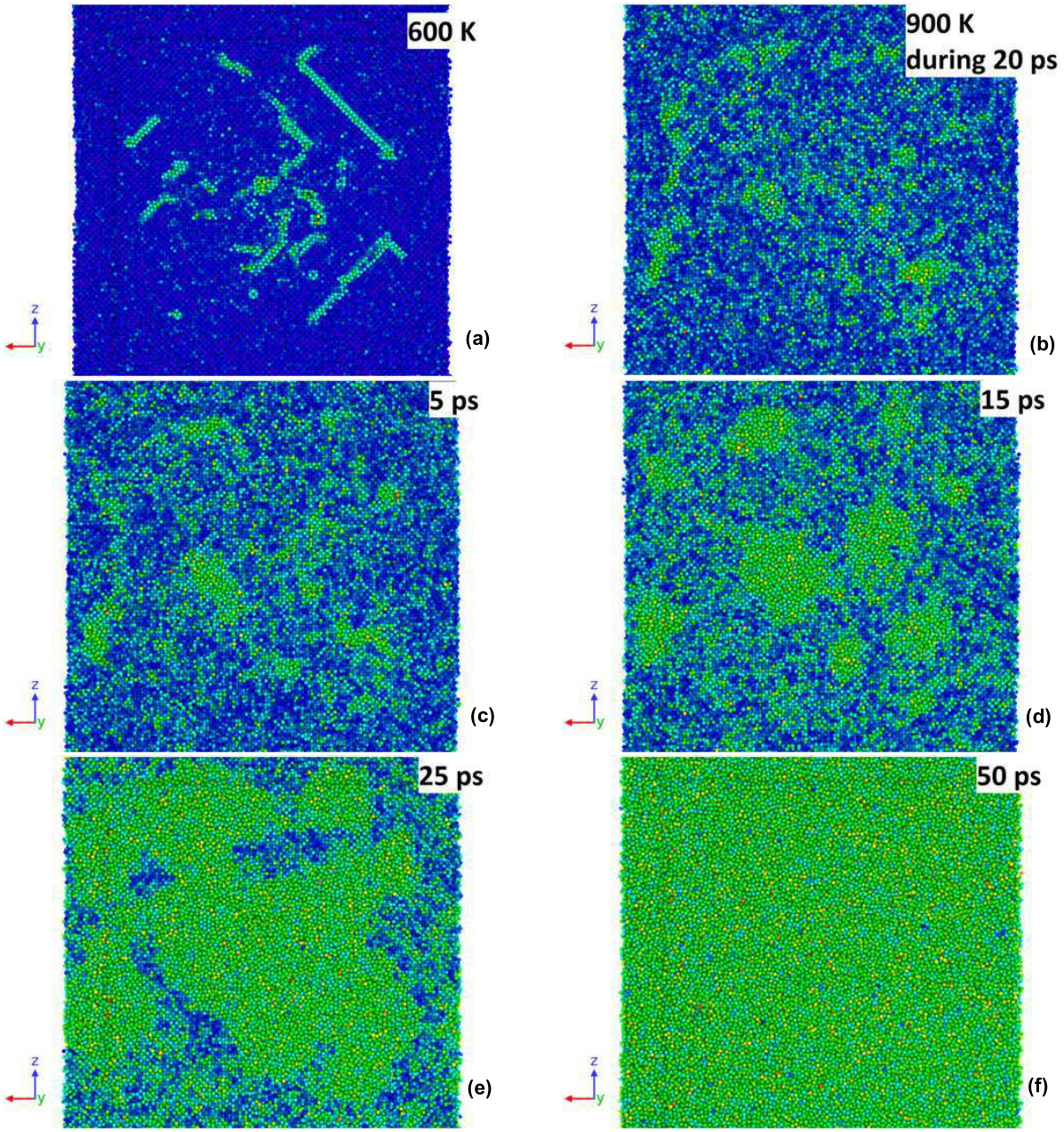

Figure 6. Melting of aluminum containing initial dislocation network. Initial dislocation structure at 600 K and defect structure formed during 20 ps at 900 K are shown in first two inserts. Various moments of time are presented under heating with constant rate of 15 PW/kg. Atoms of solid are primarily colored by blue, liquid—by green.

differ from the previously mentioned calculation results with perfect lattice for all rates of heat supply (figure 8), but decreasing of the heating rate leads to increase of this difference, so the maximum difference in data is not greater than 1% for 35.1 PW/kg rate, difference is not more than 2% for 14.5 PW/kg and it is not more than 3% for 7 PW/kg.

In the case of pre-existing dislocation network the transformation of the dislocation subsystem occurs during the thermostating of system at 900 K for 20 ps: spherical clusters of atoms with a defect environment are formed instead of plane stacking faults (figure 6). Further, these clusters

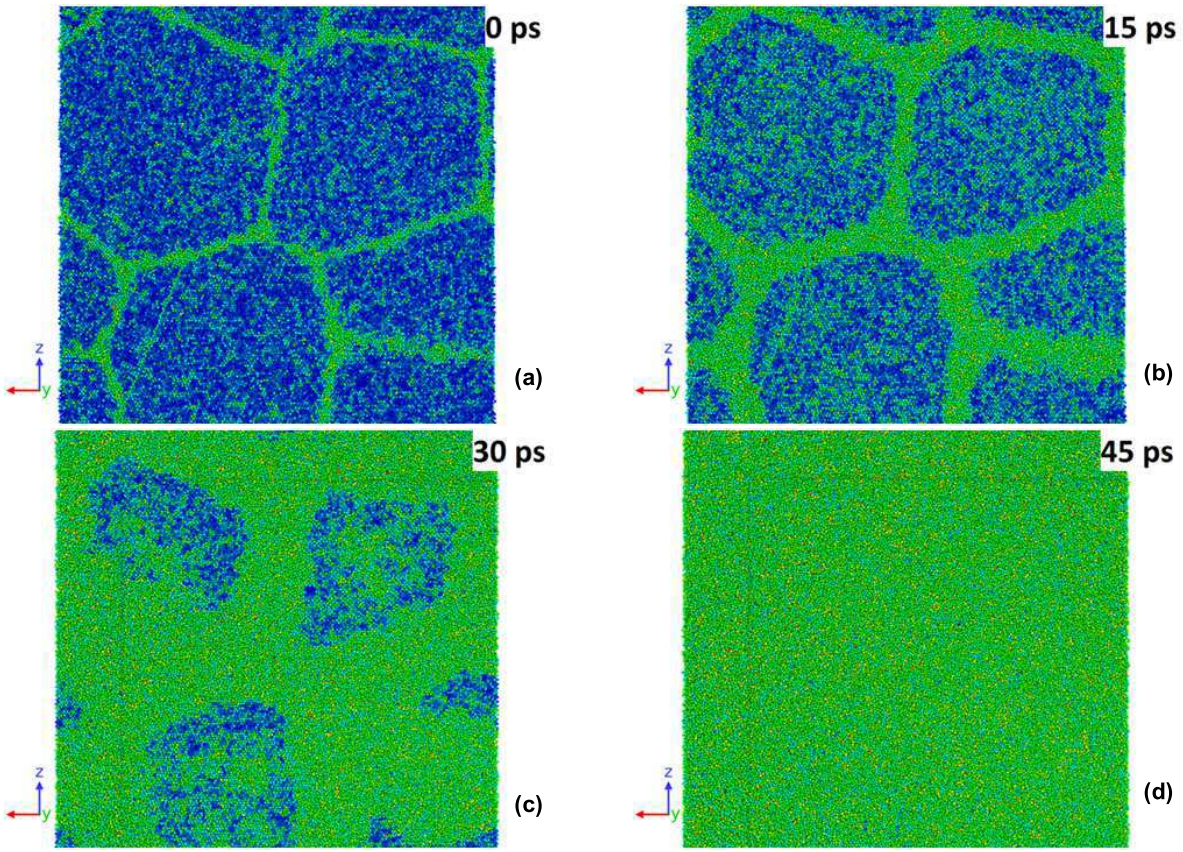

Figure 7. Melting of aluminum containing initial grain boundaries. Various moments of time are presented under heating with constant rate of 15 PW/kg. Atoms of solid are primarily colored by blue, liquid—by green.

act as centers of melting, the boundaries of the material, which is undergone a phase transition, extend due to growth of these centers and other nuclei of the liquid phase are practically not formed. The dependencies of temperature on time for these systems demonstrate a significant difference in comparison with the case of ideal lattice (figure 8); the difference reaches 10% in the point of maximal temperature for heating rate of 7 PW/kg.

In the simulations with systems containing grain boundaries the melting always starts at these boundaries (figure 7) and propagates from the boundaries deep into the grain gradually filling the entire volume of the modeled system. Similar behavior was observed in [14], where the melting of nanocrystalline copper was studied. Time dependencies of temperature exhibit the maximal difference in comparison with the case of ideal lattice; under the heating with 14.5 PW/kg rate the temperature-time curve demonstrates the monotonic increase of temperature without inflections corresponding to the substance overheating and following full melting (figure 8).

Both observed tendencies to the decrease in the difference between the maximal and minimal values of temperature depending on the increase in the degree of initial defect atoms number and on the decrease of heating rate can be explained as follows. In the case of an ideal lattice the overheating of substance results in the rapid formation of critical melting nuclei in the volume of the area that leads to the formation of large number of centers absorbing energy for the latent heat of melting. As a result, there is a significant decrease in the temperature of the material. In the presence of defect areas in system such overheating does not occur, melting is locally activated much earlier, which is evidenced by the earlier deviation of temperature rise curves

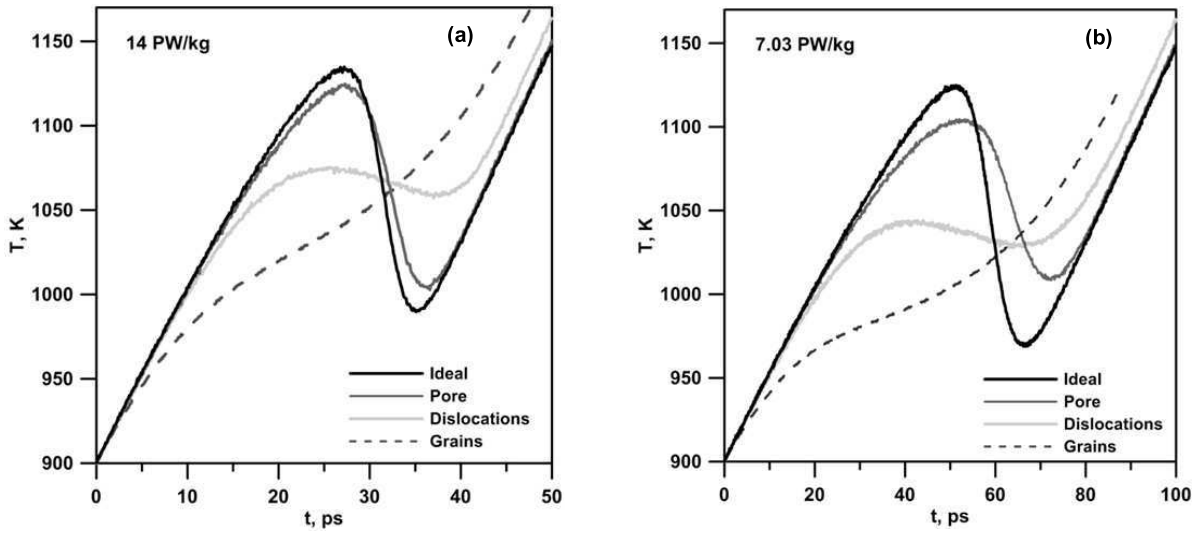

Figure 8. Melting curves for aluminum under heating with two constant rates. Data for ideal lattice and defects containing systems (void, dislocation network, grain boundaries) are given.

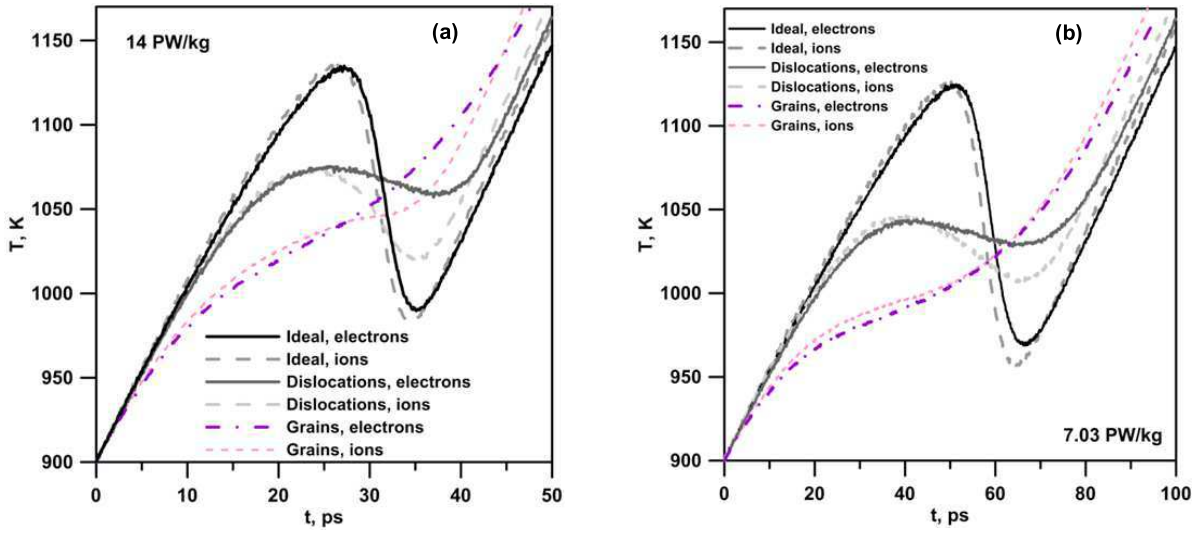

Figure 9. Comparison of data for melting curves obtained in calculations with ("electrons" in captions) and without ("ions" in captions) electronic heat conductivity.

for regions with defects from the curve for ideal lattice simultaneously with an increase of defect atoms degree. Therefore, the phase transition occurs more smoothly; and for system with grain boundaries the overheating does not take a place at middle rate of heating, further decrease the heating rate only increases this trend.

When calculations without taking into account electronic thermal conductivity are performed, the tendency similar to the case of an ideal lattice is observed. Reduction of thermal conductivity in the system weakly affects the temperature of overheating of fixed system, but the difference in subsequent decrease of temperature after activation of melting in systems with defects manifests itself in a greater extent compared with the case of an ideal lattice (figure 9). In the systems with grain boundaries the maximum in temperature-time curve is absent, but the difference here is distinguishable, particularly well when the heating occurs with the middle and maximum

rate. The temperature-time dependencies demonstrate more substantial bending in comparison with the case of accounting electronic conductivity.

It should be noted that the observed systems possess the sufficiently high initial imperfection degree, which typically has a significantly lower value in real solids. Thus, the effect of the temperature drop during the phase transition can probably be registered at the realistic rates of heating, for example, by the electronic or laser irradiation and at the real degree of the metal defectiveness.

4. Conclusions

The MD study of the non-equilibrium melting of aluminum are carried out in three model statements: (i) establishment of the equilibrium in the isolated system with a flat interface between solid and liquid phases; (ii) melting of the initially uniform single crystal under heating with a constant rate; and (iii) melting of systems containing the initial defect structure at a constant heating rate. Analysis of the obtained results shows that, when the melting front propagates, the transformation of material structure requires negligible time and that velocity of the front movement is determined by the rate of heat supply or removal from it. Presence of defect regions in crystal leads to the reduction of overheating and to the lowering of temperature dip behind the maximum on temperature-time curves compared to the case of an ideal lattice due to an earlier activation of melting at initial lattice defects and due to later completing of phase transition from the smaller number of the phase transition sites.

MD simulations are carried out both including and excluding the electronic subsystem. Accounting for electronic subsystem does not affect the value of overheating, which is achieved during the heating at a constant rate of energy release, neither in systems with an ideal lattice nor in systems with defects. At the same time, the behavior of temperature-time dependencies after achievement of temperature maximum significantly varies in these systems; in the case of calculations with electronic heat conductivity the curves demonstrate a smoother character due to distribution of the latent heat of melting over the all volume of the system.

Acknowledgments

Authors are grateful to S V Starikov for useful discussion about the parameters of electronic heat conductivity model and about the implementation of TTM library into LAMMPS.

The work was supported by the grant from the Russian Foundation for Basic Research (project No. 15-32-21039).

References

[1] Ashitkov S I, Agranat M B, Kanel G I, Komarov P S and Fortov V E 2010 *JETP Lett.* **92** 516–520
[2] Abrosimov S A, Bazhulin A P, Voronov V V, Geras'kin A A, Krasyuk I K, Pashinin P P, Semenov A Y, Stuchebryukhov I A, Khishchenko K V and Fortov V E 2013 *Quantum Electron.* **43** 246–251
[3] Inogamov N A, Zhakhovsky V V, Petrov Y V, Khokhlov V A, Ashitkov S I, Khishchenko K V, Migdal K P, Ilnitsky D K, Emirov Y N, Komarov P S, Shepelev V V, Miller C W, Oleynik I I, Agranat M B, Andriyash A V, Anisimov S I and Fortov V E 2013 *Contrib. Plasma Phys.* **53** 796–810
[4] Nie B, Huang H, Bai S and Liu J 2015 *Appl. Phys. A* **118** 37–41
[5] Dudarev E F, Markov A B, Mayer A E, Bakach G P, Tabachenko A N, Kashin O A, Pochivalova G P, Skosyrskii A B, Kitsanov S A, Zhorovkov M F and Yakovlev E V 2013 *Russ. Phys. J.* **55** 1451–1457
[6] Gnyusov S F, Rotshtein V P, Mayer A E, Rostov V V, Gunin A V, Khishchenko K V and Levashov P R 2016 *Int. J. Fract.* **199** 59–70
[7] Povarnitsyn M E, Fokin V B and Levashov P R 2015 *Appl. Surf. Sci.* **357** 1150–1156
[8] He A M, Wang P, Shao J L, Duan S Q, Zhao F P and Luo S N 2014 *J. Appl. Phys.* **115** 143503
[9] Shao J L, Wang P, He A M, Duan S Q and Qin C S 2013 *J. Appl. Phys.* **113** 163507
[10] Levitas V I and Ravelo R 2012 *Proc. Natl. Acad. Sci. U. S. A.* **109** 13204–13207
[11] Lutsko J F, Wolf D, Phillpot S R and Yip S 1989 *Phys. Rev.* B **40** 2841–2855
[12] Morris J R, Wang C Z, Ho K M and Chan C T 1994 *Phys. Rev.* B **40** 3109–3115

[13] Sun D Y, Asta M and Hoyt J J 2004 *Phys. Rev.* B **69** 024108
[14] Kuksin A Y, Norman G E, Stegailov V V and Yanilkin A V 2007 *Comput. Phys. Commun.* **177** 34–37
[15] Maltsev I, Mirzoev A, Danilov D and Nestler B 2009 *Modell. Simul. Mater. Sci. Eng.* **17** 055006
[16] Monk J, Yang Y, Mendelev M I, Asta M, Hoyt J J and Sun D Y 2010 *Modell. Simul. Mater. Sci. Eng.* **18** 015004
[17] Gaoet Y F, Yang Y, Suna D Y, Asta M and Hoyt J J 2010 *J. Cryst. Growth* **312** 3238–3242
[18] Orekhov N D and Stegailov V V 2015 *Carbon* **87** 358–364
[19] Norman G E and Stegailov V V 2004 *Mol. Simul.* **30** 397–406
[20] Norman G E and Pisarev V V 2012 *Russ. J. Phys. Chem.* **86** 1447–1452
[21] Plimpton S J 1995 *J. Comput. Phys.* **117** 1–19
[22] Brown W M, Kohlmeyer A, Plimpton S J and Tharrington A N 2010 *J. Cryst. Growth* **312** 3238–3242
[23] Duffy D M and Rutherford A M 2007 *J. Phys.: Condens. Matter* **19** 016207–016218
[24] Duffy D M and Rutherford A M 2007 *J. Phys.: Condens. Matter* **19** 496201–496210
[25] Norman G E, Starikov S V and Stegailov V V 2012 *J. Exp. Theor. Phys.* **114** 792–800
[26] Pisarev V V and Starikov S V 2014 *J. Phys.: Condens. Matter* **26** 475401
[27] Lin Z, Zhigilei L V and Celli V 2008 *Phys. Rev.* B **77** 075133
[28] Mendelev M I, Kramer M J, Becker C A and Asta M 2008 *Phil. Mag.* **88** 1723–1750
[29] Stukowski A 2010 *Model. Simul. Mater. Sci. Eng.* **18** 015012
[30] Kelchner C L, Plimpton S J and Hamilton J C 1998 *Phys. Rev.* B **58** 11085
[31] Errandonea D 2010 *J. Appl. Phys.* **108** 033517
[32] Boehler R and Ross R 1997 *Earth Planet. Sci. Lett.* **153** 223
[33] Hanstrom A and Lazor P 2010 *J. Alloys Compd.* **305** 209
[34] Lindeman F A 1910 *Z. Phys.* **11** 609
[35] Khishchenko K V 2008 *J. Phys.: Conf. Ser.* **98** 032023
[36] Khishchenko K V 2008 *J. Phys.: Conf. Ser.* **121** 022025